RESEARCH ARTICLE

Eva Neuhöferová
Romana Křivohlavá
Katrine Qvortrup Jakobsen
Veronika Benson

Authors' addresses:
Laboratory of Modulation of Gene Expression, Institute of Microbiology of the CAS, v. v. i., Prague, Czechia

Interaction of non-targeted nanodiamond carriers with specialized rodent cells: preliminary *ex vivo* and *in vivo* study

ABSTRACT

Nanodiamonds are often tested as practical drug delivery systems because they are nontoxic, biocompatible, and can easily transport various biomolecules. However, their effect on living systems has not been fully explored. In this study, we used fluorescent nanodiamonds carrying small RNA, and they were used *ex vivo* and *in vivo* to observe changes in the important cytokines TNF-α and IFN-γ. We studied the response of primary cells after contact with the loaded nanodiamond carriers. Specifically, blood, peritoneal macrophages, and spleen were examined for cytokine expression, cell internalization, and toxicity. Nanodiamonds were detected in peritoneal macrophages and spleen after *ex vivo* and *in vivo* stimulations. Cell viability was comparable in the samples with/without nanodiamond exposure in vivo. We found a significant increase in TNF-α and IFN-γ protein levels in peripheral blood mononuclear cells after stimulation with bare nanodiamonds, but no increase was measured when the same cells were exposed to RNA-loaded nanodiamonds. In addition, real-time qPCR showed no significant changes in TNF-α and IFN-γ levels after stimulation with nanodiamonds and loaded nanodiamonds *ex vivo* and *in vivo*, except for a sample of peritoneal macrophages stimulated with bare nanodiamonds. Finally, there was no significant change in hemolysis when comparing samples with nanodiamond or control stimulation. We conclude from our observations that RNA-loaded fluorescent nanodiamonds do not significantly affect TNF-α and IFN-γ levels and have minimal direct toxicity to red blood cells. However, the nanodiamond particles were found in peritoneal macrophages and spleen after *i.p.* application, suggesting the importance of targeted coating for their systemic application.

Key words: fluorescent nanodiamonds; nanodiamond carriers; RNA delivery; nanoparticles *ex vivo*; intraperitoneal application of nanoparticles

Correspondence:
Eva Neuhöferová
Laboratory of Modulation of Gene Expression, Institute of Microbiology of the CAS, v. v. i., Prague, Czechia
Tel.: +420296442395
e-mail eva.neuhoferova@biomed.cas.cz

Article info:
Received: 5 April 2022
Accepted: 21 January 2022

Introduction

Because of their properties, nanodiamonds have shown to be potentially beneficial carriers of drugs or other commodities (Fu, 2007; Holt, 2007; Alhaddad, 2012; Mochalin, 2012). Nanodiamond carriers are not only chemically inert and nontoxic, but they also have high biocompatibility with living cells (Paget, 2014) and presumably with whole organisms (Zhu, 2012). Fluorescent nanodiamond (FND) carriers are able to efficiently transport cargo inside cells and can be visualized thanks to their fluorescence, which does not fade or blink (Petrakova, 2015). Nitrogen vacancies (NVCs) located in the crystal lattice of FNDs give them their fluorescence. When exposed to a laser beam of 559 nm, they emit a far-red light signal in the range of 600 to 700 nm (Chang et al., 2008; Liu, 2009). NVC, and thus the fluorescence of the nanodiamonds used in this research, was produced by high-energy (15.5 MeV) proton irradiation of nanodiamonds. The nanodiamonds used in this research are 35-50 nm in size and their surface Z-potential is negative. A cationic polyethyleneimine (PEI) linker with a size of 800 kDa was used to effectively load small RNA molecules. This method has already been shown to be an efficient approach for transporting short oligonucleotides (Zhang, 2009). For the same purpose, we have developed a nanodiamond carrier that can transport molecules into the cytoplasm of specialized cells while allowing real-time monitoring of the transport (Petrakova, 2016). Delivery of RNA into the cytoplasm of the cell by FND carriers showed to be effective and harmless in our previous in vitro research (Lukowski & Neuhoferova, 2018).

Although nanodiamonds appear to be a promising delivery system and have many beneficial properties, they pose a potential threat in terms of their toxicity in vivo. Nanodiamonds can accumulate in various tissues, including immune cells and the reticuloendothelial system. Therefore, we decided to study the response of primary cells after the introduction of loaded nanodiamond carriers.

Blood cells, peritoneal macrophages, and spleen-derived samples were studied after the application of FND and RNA-loaded FND in both *ex vivo* and *in vivo*.

Materials and Methods

Nanoparticle handling

Preparation of nanodiamond complexes

Nanodiamond particles with fluorescent nitrogen-vacancy centers (FND) were kindly provided by Dr. Vladimira Petrakova (Faculty of Biomedical Engineering, Czech Technical University, Kladno, Czech Republic) in 2 mg/ml deionized water solution. The coating of FND particles was described in our previous report by Lukowski et al. in 2018. Briefly, before each manipulation, FNDs were subjected to ultrasonic treatment in an ice water bath for 30 min. Polyethylenimine (PEI) with a molecular weight of 800 kDa, diluted to a concentration of 0.9 mg/ml, was added to the FNDs, and the mixing ratio (v/v) of both components was 1:1. The complex of FND and polymer was stirred overnight and then centrifuged (9000 g at 4 °C) for 60 min. Unbound PEI molecules were discarded by removing the supernatant. The complex was then diluted with deionized water to maintain the originally added concentration of 1 mg/ml FND. The dissolved pellet was then sonicated for 20 minutes and mixed with a sequence of antisense microRNA 135b (A135b) (5' UptCptAptCAUAGGAAUGAAAAGCCptAptUptA 3') synthesized and modified by IDT at a concentration of 0.27 mg per 1 mg FND input weight. The total complex of FND, polymer, and RNA (FND-PEI-RNA) was mixed well and incubated for 1 hour at room temperature.

Characterization of nanodiamonds

The nanodiamond particles used in this study were previously characterized in terms of their size, charge, and dispersity using a Zetasizer Nano ZS (Malvern Instruments, Milcom) at the University Centre for Energy Efficient Buildings (UCEEB, Czech Technical University in Prague). The hydrodynamic diameter (Z-average) and polydispersity index (PdI) were measured at a scattering angle of 173° at 25 °C using dynamic light scattering (DLS) before and after coating. The analysis was performed using Zetasizer software 7.11 (Malvern Instruments, Milcom).

Atomic force microscopy (AFM) was used to visualize the nanodiamond complex in comparison with the pure nanoparticles and the PEI 800 coated nanoparticles. AFM measurements were performed at the J. Heyrovsky Institute of Physical Chemistry, Czech Academy of Sciences. Dimension Icon AFM from Bruker was used to measure the size of the nanoparticles, while PeakForce tapping mode and ScanAsyst silicon nitride probes (set point 1 nN) were used.

Ex vivo analyzes

Hemolysis

The degree of hemolysis was measured to investigate the damage to red blood cells after stimulation with nanodiamonds and nanodiamond complexes. Blood was isolated from three healthy C57BL/6 animals. Animals were anesthetized with a combination of ketamine and xylazine, we used 100 mg/kg Narkamon 5% (Bioveta, 50 mg/ml ketamine) and 10 mg/kg Rometar 2% (Bioveta, 20 mg/ml xylazine). Peripheral blood was obtained by cardiac puncture, and animals were then euthanized by cervical dislocation. Approximately 400 µl of peripheral blood was obtained, diluted 10-fold with RPMI-1640 medium (Sigma, Life Sciences), and seeded onto flat-bottom 96-well culture plates (JET BIOFIL). Nanodiamonds and nanodiamond complexes were added to the cells at a concentration of 25 µg of bare nanodiamond per 1 ml of medium. Cells were treated with phosphate-buffered saline (PBS) for the negative control sample and with ACK Lysing Buffer (Gibco™) for the positive control sample. At 60 min post-stimulation, absorbance was measured using the Infinite 200 PRO multimode plate reader (Tecan) at wavelengths from 400 nm to 620 nm.

Isolation and incubation of peripheral blood mononuclear cells

Peripheral blood mononuclear cells (PBMC) were isolated by cardiac puncture from a six-week-old C57BL/6 animal under anesthesia. Healthy animals were anesthetized with a combination of ketamine and xylazine, there were used 100 mg/kg Narkamon 5% (Bioveta, 50 mg/ml ketamine) and 10 mg/kg Rometar 2% (Bioveta, 20 mg/ml xylazine). Peripheral blood was collected and animals were then euthanized by cervical dislocation. Approximately 400 µl of peripheral blood was mixed with 200 µl of 5 mM EDTA, diluted with PBS (to a final volume of 4 ml), and carefully layered onto 3 ml of Ficoll-Paque PREMIUM 1.084 (GE Healthcare). Samples were then centrifuged at 400 g for 35 minutes, and the top layer containing plasma and platelets was discarded. The layer containing the PBMCs was transferred to a sterile tube, diluted with phosphate-buffered saline to a final volume of 6 ml, and centrifuged twice at 400 g for 10 minutes. The pellet containing the cells was then resuspended in RPMI-1640 medium (Sigma, Life Sciences) containing 10% (v/v) fetal bovine serum (FBS, Gibco™) and 44 mg/l gentamicin (Sandoz, Novartis Company). Prior to stimulation with nanodiamond complexes, cells were incubated in Petri dishes for 2 days under air-saturated and humid conditions (37 °C, 5% CO2). GolgiStop (BD Biosciences) was added to the cells according to the manufacturer's protocol. Nanodiamonds and nanodiamond complexes were added to the cells at a concentration of 25 µg of nanodiamonds per 1 ml of medium.

Intracellular staining for flow cytometry

First, we fixed the PBMCs obtained by the previous method. Cells were washed with PBS and 100 µl of a 4% paraformaldehyde solution was added for 20 min incubation under cooling conditions. Permeabilization solution (Perm/Wash Buffer, BD Biosciences) was used for two consecutive 2-minute washes at 4 °C. 10 µl of the antibody diluted in Perm/Wash solution was added to the cells and incubated for 30 min at 4 °C in the dark. Cells were then washed twice with 200 µl of Perm/Wash solution and resuspended with 200 µl of PBS. Fluorescence was measured using a flow cytometer (BD LSR II, BD Bioscience). APC fluorescence was detected with a 633 nm excitation laser, and PE fluorescence was detected with a 488 nm excitation laser. The samples were measured in three independent experiments.

Ex vivo application of nanodiamonds

Three six-week-old female Balb/c animal models were euthanized by cervical dislocation. The skin of the animals was retracted to expose the peritoneal wall. 5 ml of PBS was injected and aspirated to isolate cells from the peritoneal cavity. Spleens were removed from the sacrificed animals and homogenized in PBS. Cells were stored at 4 °C, centrifuged immediately after collection, and resuspended in RPMI-1640 medium (Sigma, Life Sciences) containing 10% (v/v) fetal bovine serum (FBS, Gibco™) and 44 mg/l gentamicin (Sandoz, Novartis Company). Before stimulation with nanodiamonds, cells were incubated for several hours in 96-well flat-bottom plastic plates under air-saturated and humid conditions (37 °C, 5% CO2), 5×10^4 cells/well. ND and ND-PEI-RNA were added to the cells at a concentration of 25 µg ND per 1 ml of medium. The control group of cells was treated with 10 µl of PBS.

In vivo analyzes

In vivo application of nanodiamonds

A total of nine six-week-old female C57BL/6 animal models were kept under standardized conditions during in vivo experiments. All experiments were performed according to the Czech law on animal protection and the experimental design was approved by the Czech Academy of Sciences under the number 82/2015. Following groups of animals with three animals per group were injected into the peritoneum with PBS, bare ND, or ND-PEI-RNA. Each dose of ND or ND-PEI-RNA sample contained 25 µg ND in 100 µl PBS. The control group was injected with 100 µl of PBS. Twenty-four hours after administration, the animals were euthanized by cervical dislocation. The skin of the animals was retracted to expose the peritoneal wall. 5 ml of PBS was injected and aspirated to isolate the cells from the peritoneal cavity. Spleens were removed from the sacrificed animals and homogenized in PBS. Samples were stored at 4 °C during collection.

Measurement of cell viability and confocal microscopy

Samples from the *in vivo* experiment were centrifuged and seeded in 96-well plastic plates (U-bottom) with 2×10^5 cells per well. Cells were washed twice with PBS and resuspended in 100 µl PBS. 10 µl propidium iodide was added to the cells to stain the non-viable cells. Positive cells were detected immediately after isolation and staining using a flow cytometer (BD LSR II, BD Bioscience).

For confocal microscopy, collected samples were seeded on 6-well glass-bottom plates with black walls, approximately 2×10^5 cells/well. Cells were incubated under air-saturated and humid conditions (37 °C, 5% CO2), allowing them to sit on the bottom.

Statistical analysis

Results in this article are presented as means +/- SD and were obtained in three different independent measurements unless otherwise stated. Statistical significance of differences was examined using an online tool available at http://astatsa.com/OneWay_Anova_with_TukeyHSD/. Parameters tested were analyzed using an ANOVA/post-hoc Tukey for group comparison. We considered values of $p \leq 0.05$ (*) and $p \leq 0.01$ (**) as statistically significant between the compared groups.

Results

Zeta potential, average size, and polydispersity index were measured to characterize the nanoparticles before and after coating, and atomic force microscopy was used to visualize the nanodiamonds before and after coating with RNA (Figure 1). These measurements showed proper coating with PEI and loading with RNA, while the average size of the nanoparticles increased by 6 nm after coating.

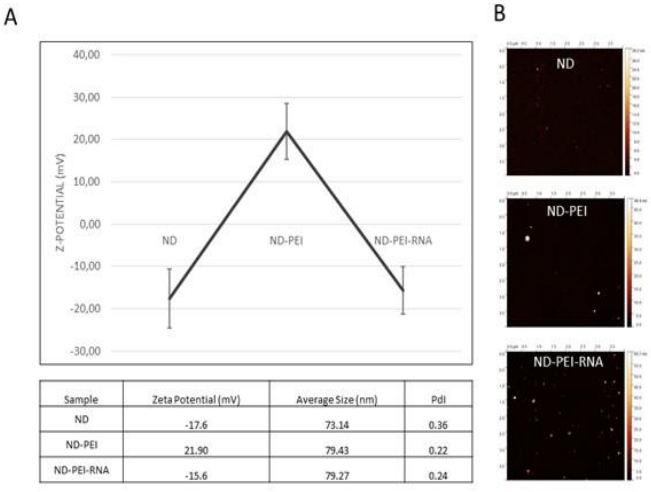

Sample	Zeta Potential (mV)	Average Size (nm)	PdI
ND	-17.6	73.14	0.36
ND-PEI	21.90	79.43	0.22
ND-PEI-RNA	-15.6	79.27	0.24

Figure 1. *Zeta-potential, average size and PdI measured on differently coated or uncoated ND is shown in A. B represents visualization of same samples using atomic force microscopy.*

Flow cytometry was used to examine the content of intracellular cytokines in PBMC incubated with FND and ND-PEI-RNA. Figure 2 shows the quantification of tumor necrosis factor alpha and interferon-gamma expression in the studied cell samples.

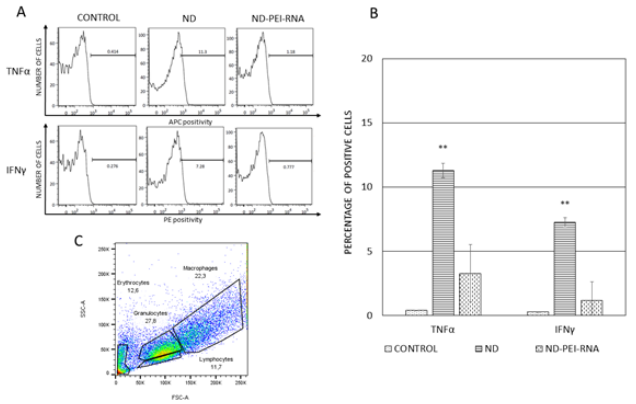

Figure 2. *Flow cytometry measurement of TNFa (APC, first row on the figure A, first bar group on the figure B) and IFNγ (PE, second row on the figure A, second bar group on the figure B) expression in PBMC cells stimulated with ND and ND-PEI-RNA complex. The value representing positive percentage of cells is set based on control sample of PBMC cells stimulated with only phosphate-saline buffer. C shows different cells populations present in PBMC sample. The data represent ex vivo experiment. The average of two measurements ± standard deviation is presented. Statistical significance of differences between tested groups was calculated by Student's t-test. Values of $p \leq 0.05$ (*) and $p \leq 0.01$ (**) were considered statistically significant.*

TNFα was detected with an antibody conjugated to allophycocyanin (APC), and IFNγ was detected with an antibody conjugated to phycoerythrin (PE). There is a significant increase in the positivity of both APC (p=0.001) and PE - (p=0.007) signals between control samples and those incubated with naked nanodiamonds. ND-PEI-RNA Stimulation resulted in non-significant changes in TNFα and IFNγ (p=0.055 and p=0.583, respectively).

Hemolysis of blood cells (Figure 3) after application of ND and ND-PEI-RNA was studied by spectrophotometry. The classical peaks of oxyhemoglobin (besides the general peak at 415 nm), which come to the fore during hemolysis, are at 540 nm and 575 nm. This analysis showed no significant changes in blood samples when comparing control, ND, and ND-PEI-RNA stimulation. Positive control represents samples treated with red cell lysis buffer (ACK buffer).

Primary cells were examined after isolation and stimulation with ND-PEI-RNA to determine the presence of nanodiamonds in the cells. Peritoneal macrophages and spleen-derived samples were isolated from animals and they were treated with ND-PEI-RNA. Figure 4 shows the confocal microscopy performed to detect the presence of internalized ND carriers *ex vivo*. The detected fluorescence was present only in peritoneal macrophages. Splenocyte samples did not exhibit a specific signal, demonstrating the presence of ND in the cytoplasm. The red signal in confocal images of splenocytes incubated in the presence of ND or ND-PEI-RNA was extracellular.

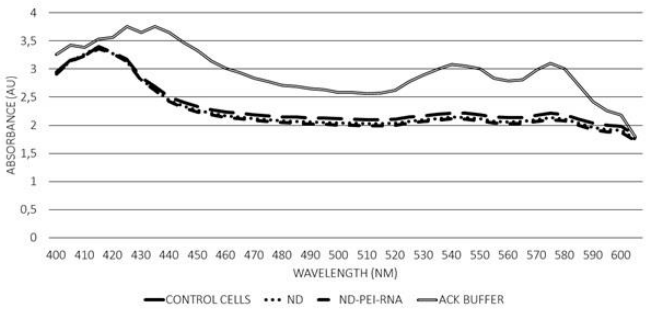

Figure 3. *Absorbance curves showing hemolysis within cell samples with different nanodiamond-based stimulation ex vivo. Absorbance is shown in arbitrary units, spectrum of absorbance wavelengths ranges from 400 to 630 nm. Specific peaks at about 415 nm refers to hemoglobin and two peaks around 540/575 nm represent lysed hemoglobin.*

The response of primary cells to the presence of bare and coated ND was also examined after intraperitoneal administration of ND or ND-PEI-RNA in vivo (Figure 5). Here we also show the percentage of live cells. Both splenocytes and peritoneal macrophages were visualized by confocal microscopy and showed similar viability (peritoneal macrophages between 64% and 70%, splenocyte samples between 61% and 70%). Peritoneal macrophages isolated from animals after *in vivo* stimulation were positive for ND and this signal was intracellular. Splenocyte samples, on the other hand, showed a positive ND signal that was extracellular.

Discussion

Fluorescent nanodiamonds show great properties as carriers of short RNAs because the surface of nanodiamond particles can be effectively coated with them (Zhang, 2009; Zhu, 2012; Petrakova, 2015). Due to their long-lasting intrinsic fluorescence, the entry of cargo into the target cell can be monitored (Liu, 2009; Petrakova, 2016; Lukowski & Neuhoferova, 2018). The nanodiamond complex carrying RNA is not toxic to the primary cells that first come into contact with it when the complex is applied to the multicellular organism (Zhang, 2009; Zhu, 2012; Paget, 2014). However, it is possible to detect the nanodiamond complex internalized into phagocytosing cells or to detect specific changes in cell morphology in response to the nanodiamond interaction.

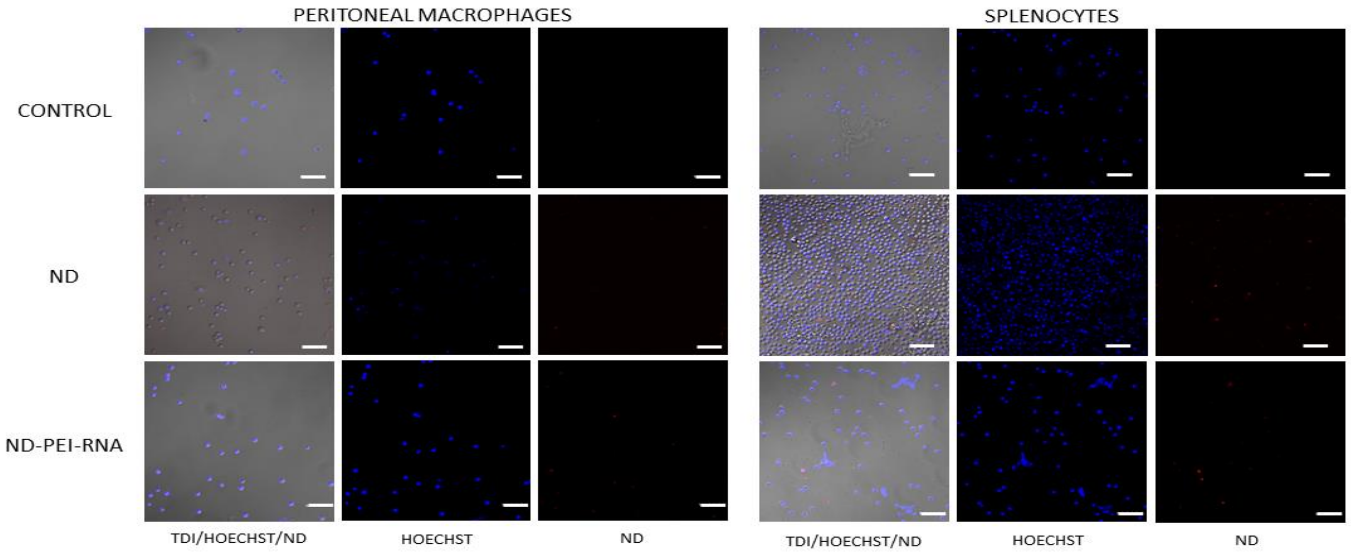

Figure 4. *Top figures show confocal microscope images of ex vivo experiment showing uptake of ND-PEI-RNA by primary cells isolated from Balb/c animals, first and third rows show images of negative control samples (PBS treatment), second and fourth row show samples of stimulation with ND-PEI-RNA for 24 hours. Scale bar represents 100 µm.*

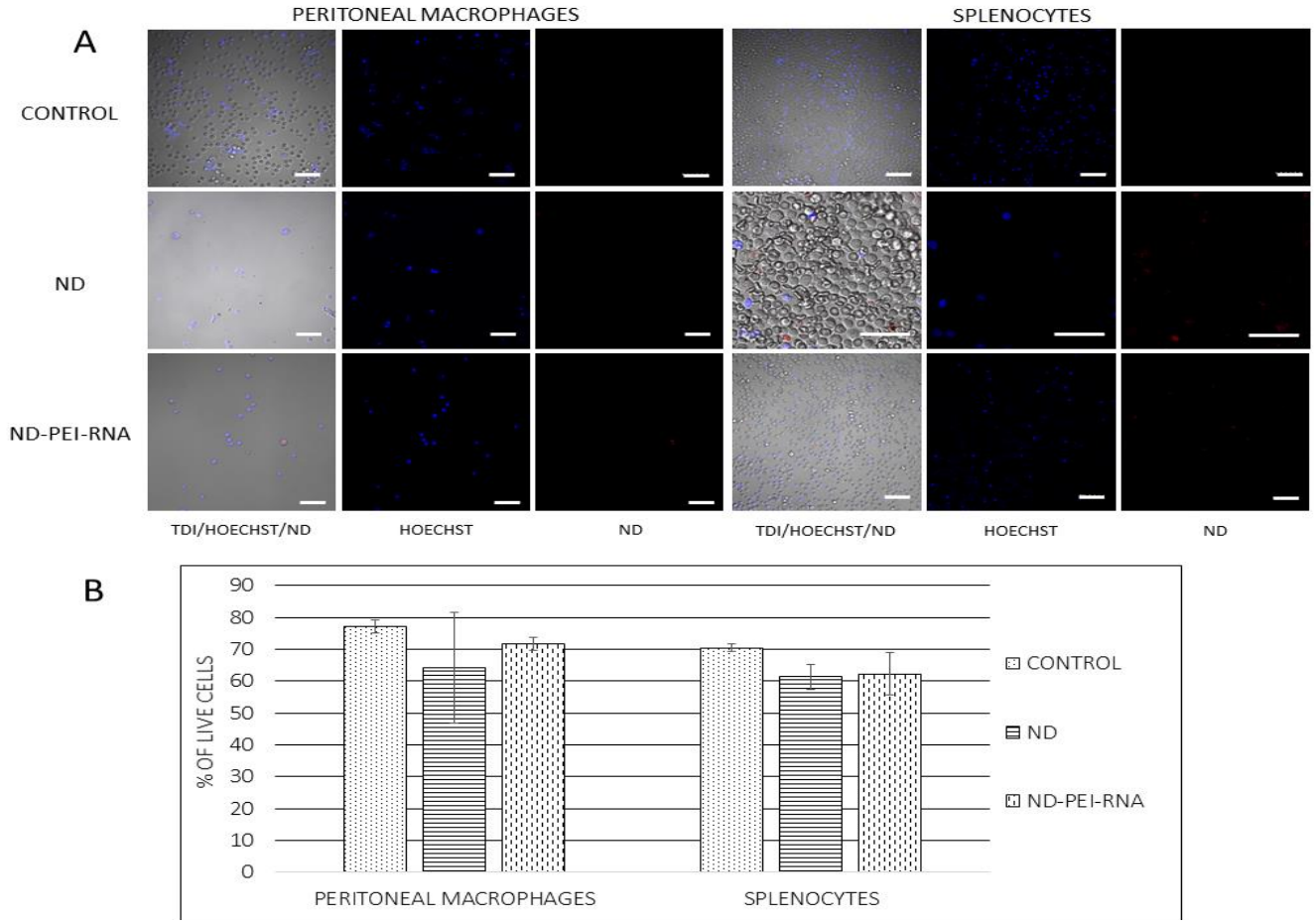

Figure 5. *Figures in A part show confocal images of peritoneal macrophages and spleen from C57BL/6 animal strain after i.p. application of bare ND and RNA-loaded ND complexes (ND-PEI-RNA). Figure B shows live cells percentage after in vivo injection of ND-PEI-RNA compared to control (i.p. PBS injection). Control stands for i.p. injection of PBS. Samples were taken 24 hours after application. Scale bar represents 100 µm. The average of two measurements ± standard deviation is presented. Statistical significance of differences between tested groups was calculated by Student's t-test. Values of $p \leq 0.05$ (*) and $p \leq 0.01$ (**) were considered statistically significant.*

This was demonstrated in our previous research where we were able to detect nanodiamonds carrying RNA in the granulocyte population of peritoneal lavage macrophages (Křivohlavá et al., 2019). In addition, Tsai et al. (2016) have shown that a high charge of naked nanodiamonds can bind to erythrocytes and decrease their oxygen transport efficiency (Tsai et al., 2016). For this reason, we decided to investigate the degree of hemolysis in blood after stimulation with our carriers. When comparing ND and ND-PEI-RNA with the control sample (no stimulation), there were no significant changes in hemolysis, indicating the compatibility of the nanodiamonds used with red blood cells. As for the positive control curve showing a shift of the primary hemoglobin peak from 415 nm to 435 nm, we assume that the measured values were too high and therefore the larger positive peak extends another 20 nm to the right.

PBMCs were stimulated *ex vivo* with bare nanodiamonds and nanodiamond complexes to detect an effect on the inflammatory cytokines TNF-α and IFN-γ.

The results shown in Figure 2 indicate that no inflammatory response is likely to be induced after binding the RNA cargo to the nanoparticle. For a more in-depth analysis of the inflammatory response, other parameters such as the major interleukins IL6, IL1, or GM-CSF need to be checked. Our preliminary analysis of TNF-α and IFN-γ suggests focusing on the effect of nanoparticle coating. In previous reports, the nanodiamond carriers also did not induce significant cytokine releases (Mohan et al., 2010; Vaijayanthimala et al., 2012; Tsai et al., 2016) and thus this result helps to shape future research on ND -bio interactions. The assessment of nanodiamond carriers in the cellular cytoplasm is important but also challenging. Detection of carriers in the cytoplasm of the target cell is a desired observation during drug delivery. However, the uptake of nanodiamond carriers by uninvolved cells is undesirable. Although nanodiamonds have shown to be generally harmless after persisting for weeks in reticuloendothelial cells or immune cells (Yuan et al., 2009; Mohan et al., 2010; Vaijayanthimala et al., 2012; Tsai et al., 2016; van der Laan et al., 2018), it would be preferable if such interaction were minimized. Macrophages naturally take up all nanoparticles from their environment (Lunov et al., 2011) and therefore we expected to find internalized ND in both *ex vivo* and *in vivo* samples from macrophages. Since we performed intraperitoneal administration, we also expected to find the nanodiamonds in the spleen (based on our previous observations not shown, we expected more nanoparticles to be taken up by the spleen than by the liver due to the mode of administration). Here, we indeed detected nanoparticles in peritoneal macrophages and there were also positive signals in samples from the spleen. In contrast to the clear intracellular location of nanodiamonds in macrophages, the positive signal in spleen samples was extracellular (Figures 4 and 5).

This could be explained by transport of the bare nanoparticles from the peritoneum to the spleen, leading to accumulation in acellular pools, by attachment of carriers to splenocytes without subsequent internalization, or by internalization and subsequent death of splenocytes in culture. We did not observe a significant difference in cell viability (Figure 5B), making the hypothesis of splenocyte death after internalization of ND unlikely.

This undesirable accumulation of nanodiamond carriers in the spleen could be overcome by a targeting molecule bound to the surface of the nanoparticles, as shown in (Křivohlavá et al., 2019). There, transferrin was used as a targeting molecule for breast tumors and achieved highly specific enrichment of nanodiamond carriers in tumor cells in contrast to RES tissue. From the data presented, we conclude that to be used as safe nanocarriers, nanodiamonds should be carefully coated with functional/effector molecules such as nucleic acid and antigen structures. We believe that this approach will reduce the nanodiamond-mediated effect on cytokine release as well as unwanted accumulation in non-targeted tissues.

Acknowledgements

The authors thank to Dr. Vladimira Petrakova (J. Heyrovsky Institute of Physical Chemistry, CAS), who executed the AFM measurements, and to Radek Divín (UCEEB, CTU in Prague) for the Zeta-sizer measurements. The authors also thank the Core of Cytometry and Microscopy (Institute of Microbiology, CAS) for confocal microscopy and cytometry measurements.

References

Alhaddad A, Durieu C, Dantelle G, Le Cam E, Malvy C, Treussart F, Bertrand JR. 2012. Influence of the internalization pathway on the efficacy of siRNA delivery by cationic fluorescent nanodiamonds in the Ewing sarcoma cell model. PLoS One, 7(12): p.e52207.

Chang YR, Lee HY, Chen K, Chang CC, Tsai DS, Fu CC, Lim TS, Tzeng YK, Fang CY, Han CC, Chang HC. 2008. Mass production and dynamic imaging of fluorescent nanodiamonds. Nat. Nanotechnol., 3(5): 284-288.

Fu CC, Lee HY, Chen K, Lim TS, Wu HY, Lin PK, Wei PK, Tsao PH, Chang HC, Fann W. 2007. Characterization and application of single fluorescent nanodiamonds as cellular biomarkers. Proc. Natl. Acad. Sci., 104(3): 727-732.

Holt KB. 2007. Diamond at the nanoscale: applications of diamond nanoparticles from cellular biomarkers to quantum computing. Philos. Trans. Royal Soc. A PHILOS T R SOC A, 365(1861): 2845-2861.

Křivohlavá R, Neuhöferová E, Jakobsen KQ, Benson V. 2019. Knockdown of microRNA-135b in mammary carcinoma by targeted nanodiamonds: potentials and pitfalls of *in vivo* applications. Nanomaterials, 9(6): p.866.

Liu KK, Wang CC, Cheng CL, Chao JI. 2009. Endocytic carboxylated nanodiamond for the labeling and tracking of cell division and differentiation in cancer and stem cells. Biomaterials, 30(26): 4249-4259.

Lukowski S, Neuhoferova E, Kinderman M, Křivohlavá R, Mineva A, Petrakova V, Benson V. 2018. Fluorescent nanodiamonds are efficient, easy-to-use cyto-compatible vehicles for monitored delivery of non-coding regulatory RNAs. J. Biomed. Nanotechnol., 14(5): 946-958.

Lunov O, Syrovets T, Loos C, Beil J, Delacher M, Tron K, Nienhaus GU, Musyanovych A, Mailander V, Landfester K, Simmet T. 2011. Differential uptake of functionalized polystyrene nanoparticles by human macrophages and a monocytic cell line. ACS nano, 5(3): 1657-1669.

Mochalin VN, Shenderova O, Ho D, Gogotsi Y. 2012. The properties and applications of nanodiamonds. Nat. Nanotechnol., 7(1): 11-23.

Mohan N, Chen CS, Hsieh HH, Wu YC, Chang HC. 2010. *In vivo* imaging and toxicity assessments of fluorescent nanodiamonds in Caenorhabditis elegans. Nano Lett., 10(9): 3692-3699.

Paget V, Sergent JA, Grall R, Altmeyer-Morel S, Girard HA, Petit T, Gesset C, Mermoux M, Bergonzo P, Arnault JC, Chevillard S. 2014. Carboxylated nanodiamonds are neither cytotoxic nor genotoxic on liver, kidney, intestine and lung human cell lines. Nanotoxicology, 8(sup1): 46-56.

Petrakova V, Benson V, Buncek M, Fiserova A, Ledvina M, Stursa J, Cigler P, Nesladek M. 2016. Imaging of transfection and intracellular release of intact, non-labeled DNA using fluorescent nanodiamonds. Nanoscale, 8(23): 12002-12012.

Petrakova V, Rehor I, Stursa J, Ledvina M, Nesladek M, Cigler P. 2015. Charge-sensitive fluorescent nanosensors created from nanodiamonds. Nanoscale, 7(29): 12307-12311.

Tsai LW, Lin YC, Perevedentseva E, Lugovtsov A, Priezzhev A, Cheng CL. 2016. Nanodiamonds for medical applications: interaction with blood in vitro and *in vivo*. Int. J. Mol. Sci., 17(7): p.1111.

Vaijayanthimala V, Cheng PY, Yeh SH, Liu KK, Hsiao CH, Chao JI, Chang HC. 2012. The long-term stability and biocompatibility of fluorescent nanodiamond as an *in vivo* contrast agent. Biomaterials, 33(31): 7794-7802.

van der Laan K, Hasani M, Zheng T, Schirhagl R. 2018. Nanodiamonds for *in vivo* applications. Small, 14(19): p.1703838.

Yuan Y, Chen Y, Liu JH, Wang H, Liu Y. 2009. Biodistribution and fate of nanodiamonds *in vivo*. Diam. Relat. Mater., 18(1): 95-100.

Zhang XQ, Chen M, Lam R, Xu X, Osawa E, Ho D. 2009. Polymer-functionalized nanodiamond platforms as vehicles for gene delivery. ACS nano, 3(9): 2609-2616.

Zhu Y, Li J, Li W, Zhang Y, Yang X, Chen N, Sun Y, Zhao Y, Fan C, Huang Q. 2012. The biocompatibility of nanodiamonds and their application in drug delivery systems. Theranostics, 2(3): p.302.